

**DEVELOPMENT OF AN OPTICAL THERMAL HISTORY COATING SENSOR  
BASED ON THE OXIDATION OF A DIVALENT RARE EARTH ION PHOSPHOR**

**Alvaro Yanez-Gonzalez<sup>1\*</sup>, [alvaro.yanez.gonzalez@gmail.com](mailto:alvaro.yanez.gonzalez@gmail.com)**

**Enrique Ruiz-Trejo<sup>1</sup>, [enrique.ruiz-trejo@imperial.ac.uk](mailto:enrique.ruiz-trejo@imperial.ac.uk)**

**Berend van Wachem<sup>1</sup>, [b.van-wachem@imperial.ac.uk](mailto:b.van-wachem@imperial.ac.uk)**

**Stephen Skinner<sup>1</sup>, [s.skinner@imperial.ac.uk](mailto:s.skinner@imperial.ac.uk)**

**Frank Beyrau<sup>2</sup>, [frank.beyrau@ovgu.de](mailto:frank.beyrau@ovgu.de)**

**Andrew Heyes<sup>3</sup>, [andrew.heyes@strath.ac.uk](mailto:andrew.heyes@strath.ac.uk)**

<sup>1\*</sup>Imperial College London, London SW7 2AZ, UK

<sup>2</sup>Otto-von-Guericke-Universität, Magdeburg 39106, Germany

<sup>3</sup>University of Strathclyde, Glasgow G1 1XJ, UK

## **ABSTRACT**

The measurement of temperatures in gas turbines, boilers, heat exchangers and other components exposed to hot gases is essential to design energy efficient systems and improve maintenance procedures. When on-line measurements, such as those performed with thermocouples and pyrometers, are not possible or inconvenient, the maximum temperatures of operation can be recorded and measured off-line after operation. Although thermal paints have been used for many years for this purpose, a novel technique based on irreversible changes in the optical properties of thermographic phosphors, can overcome some of the disadvantages of previous methods.

In particular, oxidation of the divalent rare earth ion phosphor  $\text{BaMgAl}_{10}\text{O}_{17}:\text{Eu}$  (BAM:Eu) has shown great potential for temperature sensing between 700 °C and 1200 °C. The emission spectra of this phosphor change with temperature, which permits to define an intensity ratio between different lines in the spectra that can be used as a measurand of the temperature. In this paper, the study of the sensing capabilities of a sensor coating based on BAM:Eu phosphor material is addressed for the first time. The sensitivity of the intensity ratio is investigated in the temperature range from 800 °C to 1100 °C, and is proved to be affected by ionic diffusion of transition metals from the substrate. The use of an interlayer made of zirconia proves efficient in reducing ionic diffusion and coatings with this diffusion barrier present sensitivity comparable to that of the powder material.

## INTRODUCTION

Energy efficiency has become increasingly important in recent years. In many engineering components, such as gas turbines, boilers, heat exchangers and fuel cells, efficiency is closely related to the temperature of operation. Accurate measurement of the temperature profiles on surfaces exposed to hot gases is thus essential to increase efficiency, but also to identify components that have been exposed to temperatures outside the design limits so that maintenance procedures can be applied thus reducing system failures.

Several methods are currently available to perform temperature measurements, both in real time (thermocouples, pyrometers) and after operation (thermal paints, thermal crystals). An alternative technique involves the use of thermographic phosphors, which consist of a ceramic host material doped with a rare earth element that emits phosphorescence when excited with a suitable light source. The temporal and spectral characteristics of the phosphorescent emission of these materials can be related to the temperature. These materials have been investigated for on-line temperature measurements with application to surfaces [1-4] and gas flows [5-8]. The off-line version of thermographic phosphors, which is the subject of this work, was recently devised by Feist et al. Feist, Nicholls [9]. In this new technique, irreversible changes in the optical properties of thermographic phosphors are used to record the conditions to which they have been exposed that can be read after operation. Although the sensor cannot be used again similarly to other off-line sensors, the off-line technique presents the advantage that it does not require physical or optical access to the component being measured during operation, and therefore it is simpler to implement. Off-line thermographic sensors record a measure of the thermal exposure, which is a combination of temperature and time so that steady state exposures of known duration are necessary to obtain reliable measurements.

This new technique presents some potential advantages when compared to previous methods. The ceramic material can be applied on the surfaces as water-based paints or as robust and durable coatings using industrial deposition techniques such as atmospheric plasma spraying (APS). Exposure times can thus be potentially extended to more than just a few minutes, and temperature information can then be obtained on the whole surface rather than single points. The measurement is based on objective optical properties that can be easily measured after operation with instrumentation similar to a borescope. The expertise of an operator and dismantling of the engine are thus not necessary. Furthermore, these ceramic materials do not contain any toxic components that are present for example in thermal paints,

and which are restricted by the EU REACH [10] legislation. Some studies estimate the possibility of saving up to £3m in engine development programs by using this new technique [11].

Irreversible changes in divalent rare earth ion phosphors have been previously identified, and in particular those due to oxidation of europium in BAM:Eu can be used as an indication of the temperature up to at least 1200 °C [12-15]. BAM:Eu is a highly efficient phosphor commonly used as the blue emitter in fluorescent lamps and plasma display panels (PDPs) [16-18]. Given its availability as a standard product and its high quantum efficiency it has been used as a thermographic phosphor both in the on-line and off-line versions [6, 12-14, 19, 20].

In the present paper, BAM:Eu has been deposited as a thermal history sensor coating by the screen printing method onto Inconel 625 substrates, and its temperature sensing capabilities have been investigated in the range from 800 °C to 1100 °C. Ionic diffusion of elements from the substrate alloy into the BAM lattice has been identified in single-layer coatings by means of spectroscopy and material characterisation techniques. Element diffusion, which was responsible for variations in the optical properties of the phosphor coating due to quenching of the europium emission and appearance of new emission lines, was prevented by the use of a suitable diffusion barrier. The successful application of a zirconia-based layer as a diffusion barrier has been demonstrated and the sensitivity achieved with dual-layer coatings was comparable to that of the commercial powder.

## **METHODS**

### **Coating Manufacture**

The coatings used in this study were manufactured by the screen printing method. In this technique, the first step consists of the preparation of an ink that contains the ceramic powder, which is then deposited onto the substrate. The ceramic powder (KEMK63 UF-P1, Phosphor Technology), also referred to as solid, was first ball milled in a planetary ball mill (Retsch PM100) for 1 hour at 500 rpm. The milling media were YSZ balls of 5 mm in diameter. 2.5 mg/(m<sup>2</sup> of solid) of dispersant (Hypermer KD15) were then added to the powder with ethanol. The mixture was then ground and dried. The solvent (Terpineol) was measured separately and placed in the final container. The amount of solvent needed is that which makes the ink to be composed of 75 wt % of solid. The amount of binder (ECN7) was measured to be 2 wt % of solid and it was then added to the solvent while continuously stirring. The mixture of the solid and the dispersant was then slowly added to the container

while stirring. An additional 1 ml of solvent was normally added if the mixture became too thick.

Once the components were completely mixed, the ink was introduced in an ultrasonic bath for 20 minutes to eliminate agglomerates. If lumps were still observed, the ink was then passed through a triple roll mill for 20 minutes. After that, the ink was stored in a refrigerator.

The ink was printed onto the substrate (Inconel 625 10x10x1 mm tiles) through a screen (8x10 325 45° 5m E04 EXP, MCI Precision) with a 20x20 mm square as the printable area. The ink was at room temperature before deposition. After a single layer was printed, the sample was placed inside an air furnace at 100 °C for several hours to dry. After drying, a second layer could be printed on top of the previous one if required.

Once all the required layers were printed, the samples were sintered at 1150 °C for 2 hours in a reducing atmosphere (10 % of H<sub>2</sub> and 90 % of N<sub>2</sub>) to avoid oxidation of the Eu ion. In order to avoid delamination, the heating and cooling rates were kept at 3 °C/min.

## Characterisation

**Luminescence.** The luminescence properties of the samples were examined at room temperature with the set-up shown in Figure 1. Excitation of the samples was achieved by using the fourth harmonic (266 nm) of a pulsed Nd:YAG laser (Quanta-Ray LAB-150, Spectra Physics), with a repetition rate of 10 Hz and a pulse width of 5-7 ns. The laser energy was maintained constant at approximately 1 mJ/pulse, as measured by an energy meter (PEM-45K, Radiant Dyes), and the laser spot diameter was fixed to 4 mm.

The emission spectra of the samples were recorded by a Czerny-Turner spectrometer (Acton SP-2300i, Princeton Instruments). The spectrometer had a focal length of 300 mm and a grating with 300 g/mm. The light was collected by a 50 mm Nikon lens and focused onto the entrance slit of the spectrometer. The slit width was of 100 µm so that the resolution of the spectra was better than 1 nm. At the exit of the spectrometer, a CCD array camera (Imager Intense, LaVision) was placed at the focal plane to collect the dispersed light with an exposure time of 1 ms, which was sufficient to collect the whole phosphorescent emission. 75 single-shot spectra were recorded which were used to compute the intensity ratio statistics. The spectra were wavelength calibrated by using the narrow emission lines of a mercury lamp, and their intensity corrected for the response of the system by using the calibrated emission spectrum of a Tungsten lamp.

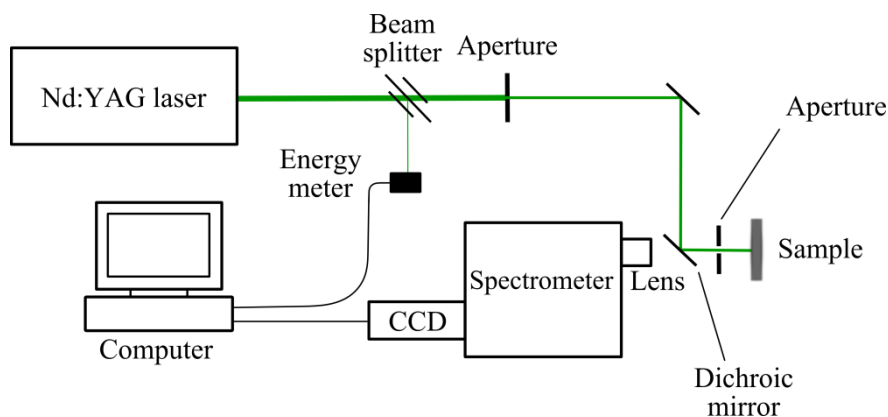


Figure 1. Schematic of luminescence detection set-up.

**Material characterisation.** The coatings manufactured in this work were examined by Scanning Electron Microscopy (SEM) and X-Ray Diffraction (XRD) analysis. The SEM (S-3400N, Hitachi) permits to perform semi-quantitative Energy-Dispersive X-Ray Spectroscopy (EDS), which allows estimating the elemental composition of the sample. The preparation of the coating samples for cross section analysis was crucial in order to obtain a flat surface characteristic of the coating. The samples were mounted in a black phenolic resin (Conducto-Mount, MetPrep) in a hot mounting press (CitoPress-1, Struers). This resin wraps the coating and makes easier the following processes of grinding and polishing the sample surface. Since the resin is conductive, it also facilitates the SEM analysis by reducing the charging effects. The sample surfaces were ground using silicon carbide paper from a grit size of 400 to 2500, and finally polished using a monocrystalline diamond suspension (down to 3  $\mu\text{m}$ ).

XRD analysis was performed in a bench machine (D2 Phaser, Bruker) that uses  $\text{CuK}\alpha$  radiation (1.5418  $\text{\AA}$ ) and permits the scanning  $2\theta$  angles from  $5^\circ$  to  $90^\circ$ .

## RESULTS AND DISCUSSION

### Powder preliminary studies

The emission spectra of BAM:Eu after heat treatment in air at various temperatures from  $800^\circ\text{C}$  to  $1200^\circ\text{C}$  is shown in Figure 2. The spectra consists of a broad band peaking at about 445 nm, due to the  $4f^65d \rightarrow 4f^7$  transitions of  $\text{Eu}^{2+}$ ; and a series of narrow peaks from 575 nm to 725 nm, due to  $^5\text{D}_0$  to  $^7\text{F}_{0,1,2,3,4}$  transitions of  $\text{Eu}^{3+}$ . Emission intensity of  $\text{Eu}^{2+}$  decreases with the heat treatment temperature, while the emission intensity of  $\text{Eu}^{3+}$  increases accordingly. The mechanisms by which these changes occur are mainly related to the process of oxidation undergone by Eu ions, and they have been studied in detail in other publications [12-14, 21, 22]. A suitable temperature measurand can be defined as the intensity ratio ( $\rho$ )

between the most intense peak of the  $\text{Eu}^{3+}$  emission located at 611 nm and the broad band emission peak of  $\text{Eu}^{2+}$  at 445 nm. This ratio increases continuously from temperatures of 800 °C up to 1200 °C for the commercial powder used in this study as shown in Figure 3.

At temperatures below 700 °C, the emission from  $\text{Eu}^{3+}$  is very weak and cannot be reliably used to define an intensity ratio. In fact, oxidation of BAM:Eu is only reported to start above 500 °C [23]. Above 1200 °C, nearly all the  $\text{Eu}^{2+}$  emission is vanished and similarly measurements cannot be used to define the intensity ratio. However, it was demonstrated in [14] that modification of the dopant concentration affects the resistance of the phosphor to oxidation and thus can be used to tune the temperatures at which the sensor is most sensitive to changes in temperature.

In this work, the powder is ball milled as part of the process of coating manufacture in order to reduce the particle size and facilitate the deposition process. The first step in the oxidation of Eu is the adsorption of oxygen on the surface of the BAM:Eu particles [21] and is thus affected by the specific surface area of the powder. A reduction of particle size such as that caused by the milling process increases the specific surface area available and thus increases adsorption. The milled powder is therefore expected to suffer a higher degree of degradation compared to the commercial powder at the same temperature, which is confirmed by the results shown in Figure 3. The intensity ratio of the ball-milled powder after heat treatment at several temperatures in the range 800 – 1200 °C is higher in value than that of the commercial powder, but the sensitivity of the measurand remains nearly constant for both types of powders.

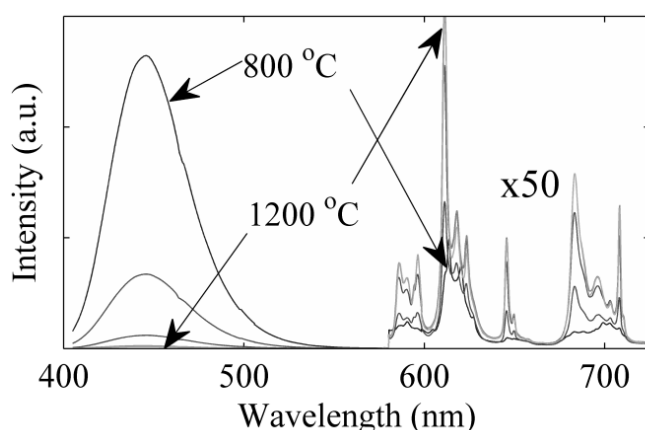


Figure 2. Emission spectra of commercial BAM:Eu samples after heat treatment at temperatures from 800 °C to 1200 °C for 20 minutes.

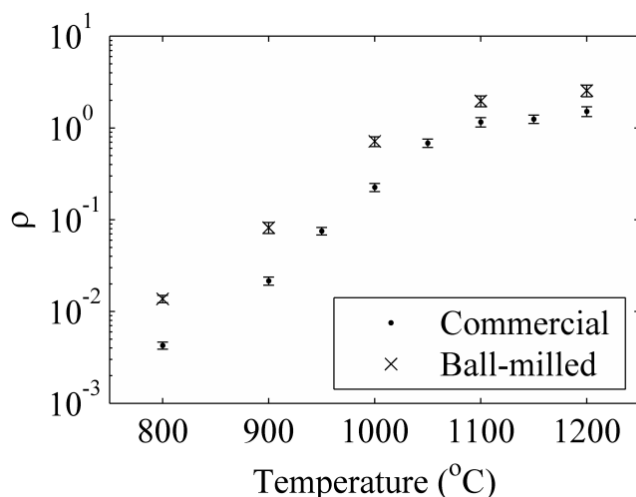


Figure 3. Intensity ratio of commercial powder and ball milled commercial powder for various heat treatment temperatures and 20 minutes exposure.

### Single-layer coating manufacture

Single-layer coatings were first manufactured by a single pass during the screen printing process. These coatings were analysed by XRD to confirm the presence of the BAM phase and the cross section examined by SEM to study the thickness and microstructure of the coatings. The diffraction patterns of the as-deposited coatings, which are shown in Figure 4, are mainly identified with the BAM phase. This indicates that no structural change in the phosphor occurs that could be identified by this technique. The diffraction peaks of the cubic phase of the substrate are also detected with lower intensity at 43.6 °, 50.8 ° and 74.6 °.

The cross-section image of the coating in Figure 5 shows a coating with an approximate thickness between 15 - 20 μm. The coating is composed of a stack of particles with multiple voids. This is caused by the relatively low temperature used in the annealing during manufacture, which is much lower than the temperature required for BAM:Eu to begin sintering. The elevated number of voids permits air to access BAM:Eu particles thus allowing adsorption of oxygen and subsequent oxidation. Therefore, the behaviour of the coating in terms of sensing capabilities is in principle expected to be similar to that of the ball milled powder.



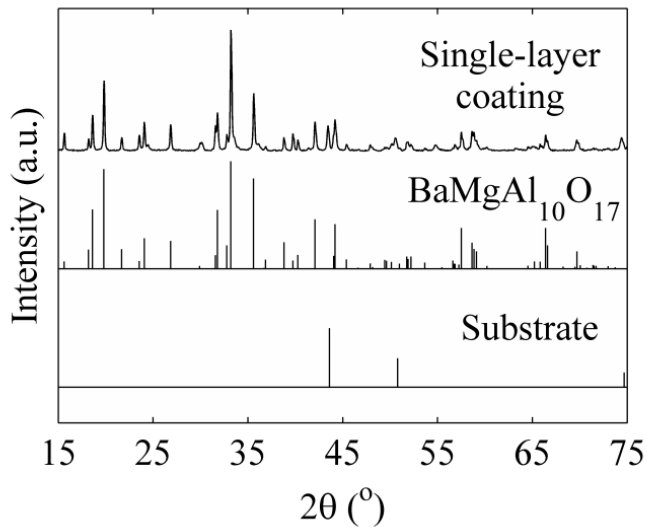


Figure 4. XRD peaks of the sample and the identified phases of BAM and nickel-based alloy substrate.

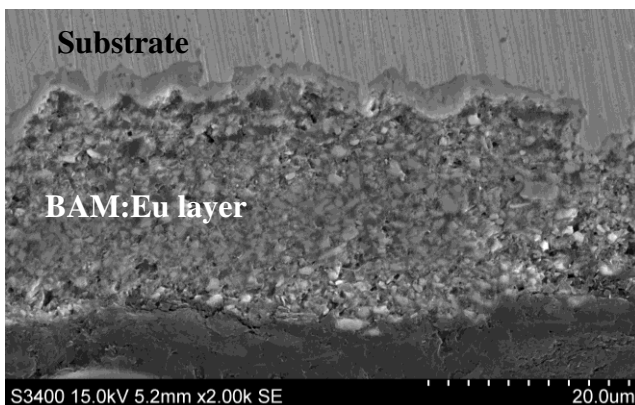


Figure 5. SEM cross-section image of the BAM:Eu screen printed coating.

### Element diffusion

Single-layer screen printed coatings were heat treated for 20 minutes in air at temperatures of 800 °C, 900 °C, 1000 °C and 1100 °C. The emission spectra of these coatings were recorded at room temperature and are shown in Figure 6 normalised to the broad band peak at 445 nm.

Emission spectra of these samples are significantly different compared to the spectra of the commercial powder heat treated in air shown in Figure 2. An emission peak at 513 nm can be now observed whose intensity increases with heat treatment temperature relative to the broad band. A similar peak at this location has been reported previously in emission spectra of

co-doped BAM:Eu,Mn [16, 24], which first suggests the diffusion of transition metal ions from the substrate alloy into the BAM lattice.

In addition to the narrow emission peaks of  $\text{Eu}^{3+}$  in the range from 575 nm to 725 nm, a broad band extending from 640 nm to at least 725 nm can now be observed, which exhibits a much larger intensity than the emission from  $\text{Eu}^{3+}$ .  $\text{Eu}^{3+}$  emission is likely to be quenched by energy transfer to the optical centres responsible for this new broad band emission. Several transition metal ions are known to emit luminescence in the red and near infra-red.  $\text{Mn}^{4+}$  emits several broad lines in the range from 620 nm to 700 nm in various host materials [25].  $\text{Cr}^{3+}$  presents emission in several hosts between 680 nm and 720 nm [25-28]. Finally,  $\text{Fe}^{3+}$  also exhibits luminescence at wavelengths above 680 nm [25, 29].

The possibility of diffusion of transition metal ions in the BAM lattice is supported by the high values of the cation mobility in  $\beta$ -alumina for  $\text{Ba}^{2+}$  and  $\text{Sr}^{2+}$ , this last one with almost the same ionic radius as  $\text{Eu}^{2+}$  [22]. Furthermore, cation mobility in the conduction layer of BAM:Eu has been previously studied with regards to thermal degradation of the phosphor [22], where diffusion of  $\text{Eu}^{2+}$ ,  $\text{Eu}^{3+}$  and  $\text{Ba}^{2+}$  ions was measured by X-ray photoelectron spectroscopy (XPS).

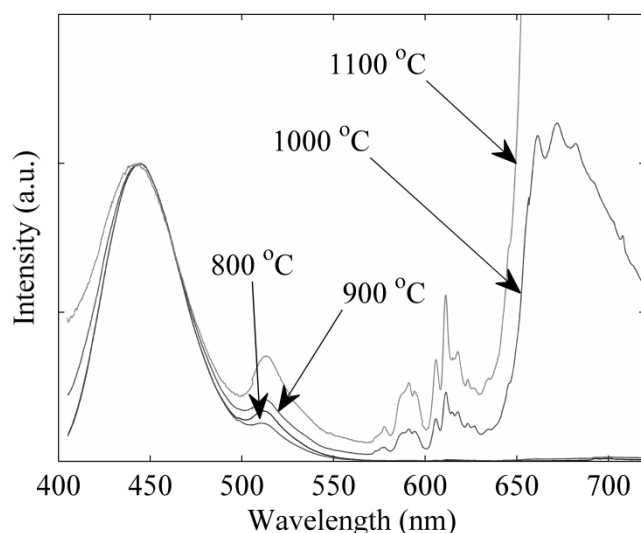


Figure 6. Normalised emission spectra of screen printed BAM:Eu single-layer coatings after heat treatment in air at 800 °C, 900 °C, 1000 °C and 1100 °C.

The diffusion of ions was further investigated by EDS analysis of the cross-section of the coating heat treated at the highest temperature of 1100 °C. The EDS spectrum was recorded at 13 different locations across the thickness of the coating. The molar content of the

detected elements was then normalised to the content of aluminium ( $Al_{10}$ ), which was considered to remain constant in the BAM lattice and the results are shown in Figure 7. This assumption is reasonable since Mn is known to substitute for Mg in the spinel block of the BAM lattice [24].  $Cr^{3+}$  and  $Fe^{3+}$  have similar ionic radii and thus are expected to occupy a similar site within the crystal lattice [30].

In Figure 7, the content of Ba oscillates around 1 mol at all locations in accordance with the chemical formula of BAM. The content of Mg is however lower than expected from the stoichiometry of BAM, and it oscillates around 0.8 mol. This could easily be explained by substitution of Mg by transition metal ions in the spinel block as mentioned before. All three elements Cr, Fe and Mn are detected by EDS. Presence of Fe and Mn is only significant at locations close to the substrate, with levels close to 0.15 mol. At distances longer than 2.5  $\mu m$  these two elements are not detected by this technique. Cr ion, however, is detected at all locations across the coating. Near the substrate, there is a steep gradient of concentration from 0.7 mol to approximately 0.13 mol at distances longer than 5  $\mu m$ , which is indicative of diffusion. Finally, the Eu content is nearly constant with a value of 0.13 mol at all positions, which is an expected value for this dopant in commercial BAM:Eu [31].

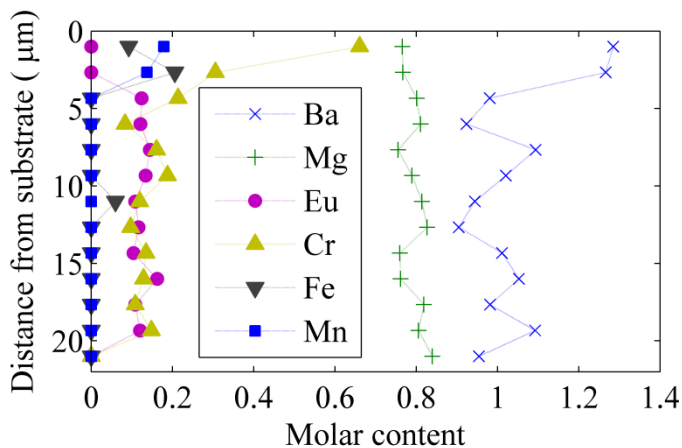


Figure 7. Molar content of various elements calculated by EDS at different locations across the thickness of the coating after heat treatment of the sample in air at 1100 °C for 20 minutes.

The results from EDS analysis confirm the diffusion of transition metal ions from the substrate into the BAM lattice. This diffusion is likely responsible for the change in the emission spectra previously observed. The peak at 513 nm can be related to the presence of  $Mn^{2+}$  after the manufacture of the coating, as shown in emission spectra in [16, 24]. However,

the broad band in the wavelength range 640 – 725 nm could be the result of contributions from  $\text{Mn}^{4+}$ ,  $\text{Cr}^{3+}$  and/or  $\text{Fe}^{3+}$ .

In order to discern the effect of each of these ions, samples were prepared by mixing 1 mg of the commercial powder with 2 wt % powder of one of each of the transition metal ions Mn, Cr and Fe. Each of the three mixtures was thoroughly ground to ensure a homogeneous mixture and then heat treated for 20 minutes in air at 1000 °C. The emission spectra of these samples were then measured at room temperature and they are shown in Figure 8 in the wavelength range from 550 nm to 725 nm. The emission spectra of the commercial powder, ball-milled powder and screen printed coatings (note that dual-layer coatings will be introduced in the following section) heat treated under the same conditions of 20 minutes exposure at 1000 °C are shown for comparison.

Analysis of spectra in Figure 8 confirms that the presence of Cr and Fe ions does not affect the emission spectrum, as these two mixtures exhibit the same emission peaks as the commercial powder alone. On the other hand, the mixture with Mn exhibits a similar emission to that of the commercial powder up to 640 nm, but an additional broad band is visible at longer wavelengths. This broad band extends over the same wavelengths as that observed in the single-layer coatings, although its intensity is much lower compared to the coating samples. This result indicates that  $\text{Mn}^{2+}$  present in fresh samples might oxidise to  $\text{Mn}^{4+}$  during the heat treatment thus giving rise to the broad band emission between 640 – 725 nm and quenching the  $\text{Eu}^{3+}$  emission.

The broadening of the  $\text{Eu}^{3+}$  emission peaks around 611 nm can be explained by the milling process. The spectra of the ball-milled powder shows much broader features at these wavelengths than that of the commercial powder. This effect is also reflected in the coating samples.

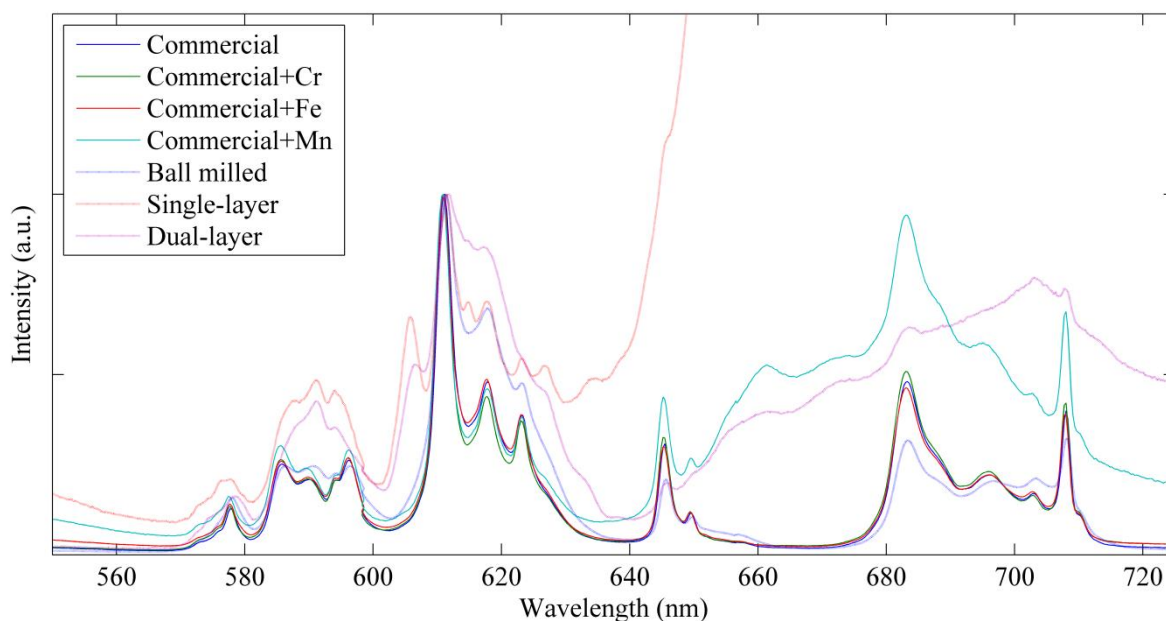


Figure 8. Normalised emission spectra of  $\text{Eu}^{3+}$  of various mixtures of commercial powder and transition metal ions, the ball-milled powder and single and dual-layer coatings.

### Dual-layer coating manufacture

A dual-layer coating was envisaged that incorporates an intermediate layer between the substrate and the phosphor coating. This layer should act as a diffusion barrier, be chemically compatible with the phosphor and the substrate and be easily deposited by screen printing. Potential candidates might be for example alumina and zirconia, being the latter selected due to the availability of a suitable ink for deposition.

A coating was manufactured by the screen printing method by first depositing a layer of Zirconia stabilised with Scandia (SSZ). On top of this layer, the BAM:Eu coating was deposited. An SEM cross-section image of this dual-layer coating is shown in Figure 9. The total thickness of this coating is of about  $14\ \mu\text{m}$ , being the SSZ layer only of about  $2\ \mu\text{m}$  and the rest corresponding to the BAM:Eu layer. The same microstructure in the phosphor layer is observed as for the single-layer coating.

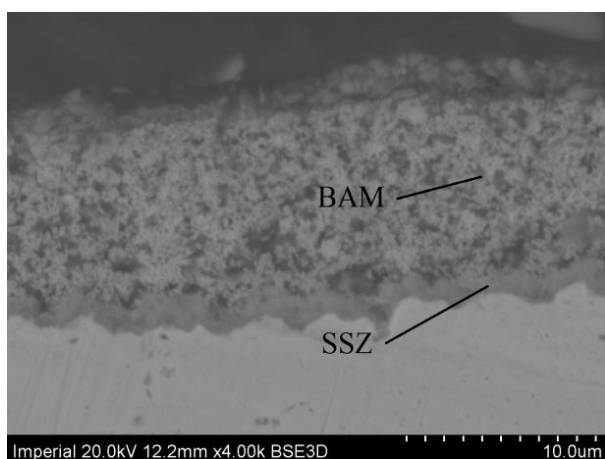


Figure 9. SEM cross-section image of the BAM:Eu screen printed coating with an interlayer of SSZ.

The emission spectrum of the coating after the manufacture process was compared to that of the single-layer coating and it is shown in Figure 10. The broad band emission corresponding to  $\text{Eu}^{2+}$  is present in both coatings, but the peak at 513 nm, which was ascribed to the presence of  $\text{Mn}^{2+}$  in the single-layer coating, is missing in the dual-layer coating. This confirms the possibility to use a SSZ interlayer to stop diffusion of transition metal ions from the substrate.

The emission spectrum of the dual-layer coating after heat treatment in air at 1000 °C, which was shown previously in Figure 8, suggests that some diffusion is still present as the broad band ascribed to emission from  $\text{Mn}^{4+}$  is clearly visible. However, the relative intensity of this broad band is drastically reduced compared to that of the single-layer coating, which indicates a much lower degree of diffusion.

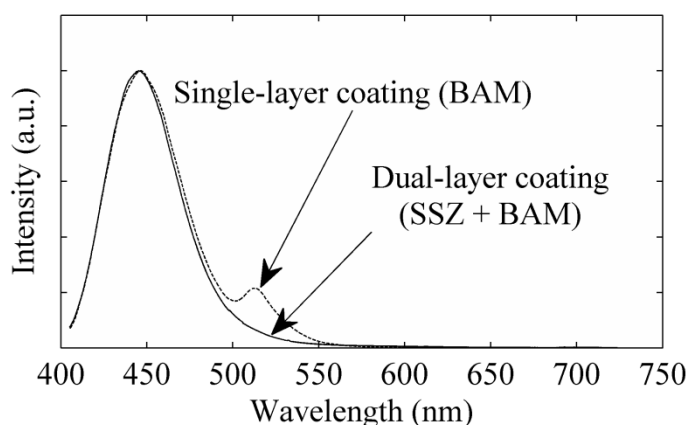


Figure 10. Normalised emission spectra of as-synthesised single and dual-layer BAM:Eu coatings.

### Comparison of intensity ratio

The diffusion of transition metal ions from the substrate causes changes in the emission spectra of coating samples. These changes affect the shape of the spectra and the relative intensities of the peaks. Therefore, temperature measurements based on the intensity ratio as defined in previous sections may be affected by this diffusion.

The intensity ratio was measured for samples whose emission spectra are plotted in Figure 8. Therefore, the intensity ratios at 1000 °C shown in Figure 11 correspond to those samples. Analysis of  $\rho$  for powder samples mixed with transition metal ions suggests that presence of Cr does not affect the value of  $\rho$ . Since the emission spectrum of this sample also showed a similar shape to that of the commercial powder, it can be concluded that Cr does not play a significant role in the luminescence process. The intensity ratio of the sample mixed with Fe has a lower value than that of the commercial powder. Therefore, although Fe does not affect the emission spectrum, it quenches the  $\text{Eu}^{3+}$  emission thus leading to a lower value of  $\rho$ . The sample mixed with Mn presents a value of  $\rho$  almost an order of magnitude lower than that of the commercial powder, which was expected by the high level of quenching observed in the emission spectrum of this sample.

The single layer coating presents a value of  $\rho$  much lower than that of the ball milled powder, which would be the expected value of  $\rho$  given the microstructure of the coating. This can be explained by the presence of both Mn and Fe in the sample. These two elements quench the emission of  $\text{Eu}^{3+}$  (and to a lower extent that of  $\text{Eu}^{2+}$ , which is reflected in overall reduced emission intensity) and thus reduce the value of  $\rho$ . The dual-layer coating prevents diffusion and thus the value of  $\rho$  is closer to the expected value of the ball-milled powder.

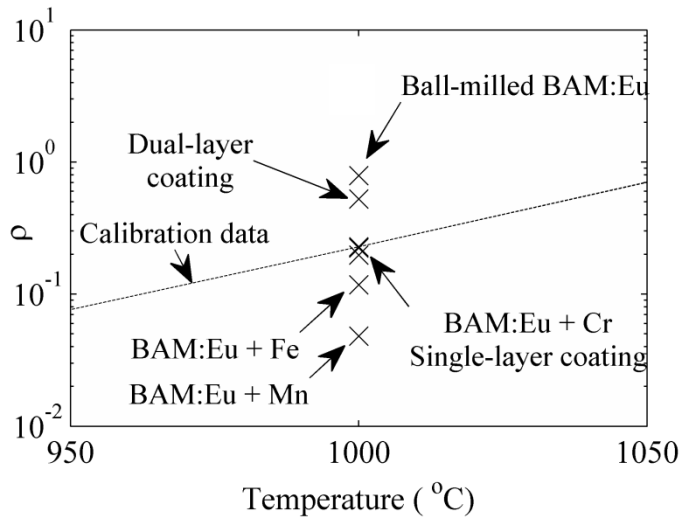


Figure 11. Intensity ratio of various mixtures of commercial powder and transition metal ions, the ball-milled powder and single and dual-layer coatings.

$\rho$  was calculated for coating samples in the temperature range 800 °C to 1100 °C and is shown in Figure 12 together with the commercial powder calibration curve. Single-layer coatings show a lower value of  $\rho$  at all temperatures. The sensitivity of these coatings is high in the temperature range between 900 °C and 1000 °C, while at other temperatures the change in  $\rho$  is relatively low compared to the commercial powder. This may suggest some change in the mechanism of degradation above 900 °C.  $\rho$  of dual-layer coatings is significantly higher than that of single-layer coatings and slightly higher than that of commercial powder (and therefore closer to the expected value of the ball milled powder). The sensitivity remains similar to that of the powder across the temperature range up to 1000 °C. At higher temperatures  $\rho$  seems to remain constant or even slightly decrease. This might be related to a higher degree of diffusion at high temperatures that is not sufficiently prevented with the thin layer of SSZ.



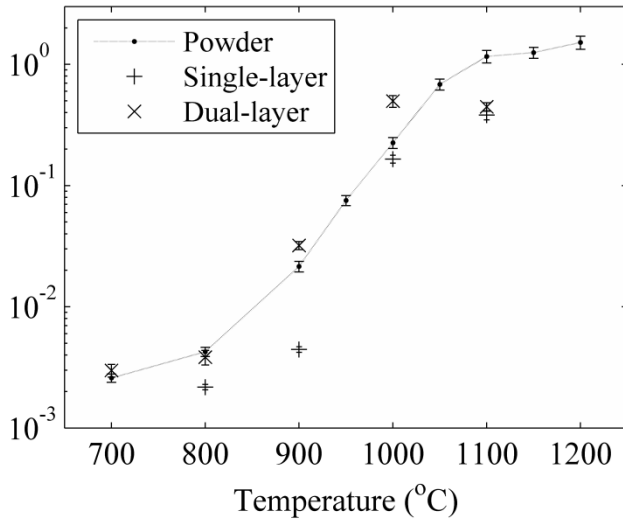


Figure 12. Intensity ratio of single and dual/layer coatings compared to the commercial powder calibration curve.

## CONCLUSIONS

Thermographic phosphor BAM:Eu has been applied as a coating sensor and the possibility to measure surface temperatures successfully demonstrated for the first time.

Single and dual-layer coatings of thermographic phosphor BAM:Eu have been deposited on Inconel 625 substrates by the screen printing method with a thickness that varied from 15 – 20  $\mu\text{m}$ . This thickness proved to be sufficient to perform luminescence measurements even after heat treatment, where the luminescence is largely reduced due to oxidation of  $\text{Eu}^{2+}$ . The microstructure of the coating consisted of a stack of particles with numerous voids, which indicates that sintering of the particles cannot be achieved at the relatively low temperatures of the annealing.

The optical characteristics of BAM:Eu coatings were investigated in the temperature range from 800 °C to 1100 °C. Emission spectra of single-layer coatings showed that, in addition to normal emission from  $\text{Eu}^{2+}$  and  $\text{Eu}^{3+}$  after heat treatment in air, an emission peak at 513 nm and a broad band extending from 640 – 725 nm was observed in the coating samples. Analysis performed by EDS and comparison of emission spectra of BAM:Eu powder samples mixed with transition metal ions (Cr, Fe and Mn) suggested that the origin of these two additional features is the presence of  $\text{Mn}^{2+}$  and  $\text{Mn}^{4+}$  respectively. However, diffusion of the other two elements was also observed although it did not affect the emission

spectra. Other minor changes in the emission spectra were ascribed to the ball-milling of the powder during coating manufacture.

The sensing capabilities of the sensor were also investigated by using the intensity ratio between the emission lines of  $\text{Eu}^{3+}$  (611 nm) and  $\text{Eu}^{2+}$  (445 nm). Analysis of powder samples heat treated at 1000 °C for 20 minutes revealed that diffusion of Mn caused a drastic reduction of the intensity ratio compared to the commercial powder. Although diffusion of Fe did not affect the emission spectra, it affected the emission efficiency and also induced a reduction in the intensity ratio. The presence of Cr showed no effect on the optical properties of the phosphor.

The emission spectra and thus the intensity ratio of single-layer coatings were greatly affected by diffusion of elements from the substrate. A dual-layer coating in which the phosphor layer was separated from the substrate by a suitable diffusion barrier was manufactured. An interlayer made of zirconia proved successful in preventing diffusion. The intensity ratio of dual-layer coatings showed a similar sensitivity to that of the powder. Therefore, the use of a diffusion barrier is essential in the performance of BAM:Eu as a sensor coating.

While the present study focuses on the intensity ratio technique, further work should look into the lifetime decay method, which has been successfully demonstrated for BAM:Eu in previous publications [14]. Additionally, the presence of transition metal ions diffusing from the substrate into the phosphor coating shown in this work is, to the knowledge of the authors, the first experimental evidence of the thermally driven diffusion mechanism described in the patent by Feist et al. Feist, Nicholls [9]. The possibility to use this mechanism to perform successful temperature measurements needs to be further investigated.

## NOMENCLATURE

BAM:Eu	Europium-doped barium magnesium aluminate ( $\text{BaMgAl}_{10}\text{O}_{17}:\text{Eu}$ )
CCD	Charge-coupled device
EDS	Energy dispersive X-ray spectroscopy
Nd:YAG	Neodymium-doped yttrium aluminium garnet
PDP	Plasma Display Panel
REACH	Registration, Evaluation, Authorisation and Restriction of Chemicals
SEM	Scanning electron microscopy
SSZ	Scandia stabilised zirconia

XPS	X-ray photoelectron spectroscopy
XRD	X-ray diffraction
$\rho$	Intensity ratio

## ACKNOWLEDGEMENTS

The authors would like to thank the financial support from The Energy Futures Lab.

## REFERENCES

1. Tobin, K., et al., *High-temperature phosphor thermometry of rotating turbine blades*. AIAA Journal, 1990. **28**(8): p. 1485-1490.
2. Allison, S.W. and G.T. Gillies, *Remote thermometry with thermographic phosphors: Instrumentation and applications*. Review of Scientific Instruments, 1997. **68**(7): p. 2615-2650.
3. Khalid, A.H. and K. Kontis, *Thermographic phosphors for high temperature measurements: Principles, current state of the art and recent applications*. Sensors, 2008. **8**(9): p. 5673-5744.
4. Feist, J., et al., *Application of an Industrial Sensor Coating System on a Rolls-Royce Jet Engine for Temperature Detection*. Journal of Engineering for Gas Turbines and Power, 2013. **135**(1): p. 012101-012101-9.
5. Omrane, A., et al., *Simultaneous 2D flow velocity and gas temperature measurements using thermographic phosphors*. Applied Physics B, 2008. **92**(1): p. 99-102.
6. Fond, B., et al., *Simultaneous temperature, mixture fraction and velocity imaging in turbulent flows using thermographic phosphor tracer particles*. Optics Express, 2012. **20**(20): p. 22118-22133.
7. Abram, C., et al., *High-speed planar thermometry and velocimetry using thermographic phosphor particles*. Applied Physics B-Lasers and Optics, 2013. **111**(2): p. 155-160.
8. Fond, B., C. Abram, and F. Beyrau, *On the characterisation of tracer particles for thermographic particle image velocimetry*. Applied Physics B, 2015: p. 1-7.
9. Feist, J., J. Nicholls, and A. Heyes, *Determining thermal history of components*, 2007.
10. REACH, *Registration, Evaluation, Authorisation and Restriction of Chemicals (REACH), Regulation (EC) No 1907/2006 of the European Parliament and of the Council*, in *OJ of the European Union L 396/1* 18.12.2006.
11. Feist, J.P., et al. *Off-Line Temperature Profiling Utilising Phosphorescent Thermal History Paints and Coatings*. in *ASME Turbo Expo 2014: Turbine Technical Conference and Exposition*. 2014. American Society of Mechanical Engineers.
12. Rabhiou, A., A. Kempf, and A. Heyes, *Oxidation of divalent rare earth phosphors for thermal history sensing*. Sensors and Actuators B-Chemical, 2013. **177**: p. 124-130.
13. Yañez Gonzalez, A., et al., *Reusable Thermal History Sensing via Oxidation of a Divalent Rare Earth Ion Based Phosphor Synthesized by the Sol-Gel Process*. Heat Transfer Engineering, 2015. **36**(14-15): p. 1275-1281.
14. Yañez Gonzalez, A., et al., *A detailed characterization of BaMgAl<sub>10</sub>O<sub>17</sub>:Eu phosphor as a thermal history sensor for harsh environments*. Sensors and Actuators A: Physical, 2015. **234**: p. 339-345.

15. Yáñez-González, Á., et al., *On the kinetics of thermal oxidation of the thermographic phosphor BaMgAl<sub>10</sub>O<sub>17</sub>:Eu*. *Materials & Design*, 2016. **108**: p. 145-150.
16. Smets, B. and J. Verlijsdonk, *The luminescence properties of Eu<sup>2+</sup>-and Mn<sup>2+</sup>-doped barium hexaaluminates*. *Materials Research Bulletin*, 1986. **21**(11): p. 1305-1310.
17. Smets, B., *Phosphors based on rare-earths, a new era in fluorescent lighting*. *Materials Chemistry and Physics*, 1987. **16**(3): p. 283-299.
18. Oshio, S., et al., *Mechanism of luminance decrease in BaMgAl<sub>10</sub>O<sub>17</sub>:Eu<sup>2+</sup> phosphor by oxidation*. *Journal of the Electrochemical Society*, 1998. **145**(11): p. 3903-3907.
19. Sarner, G., M. Richter, and M. Alden, *Investigations of blue emitting phosphors for thermometry*. *Measurement Science & Technology*, 2008. **19**(12).
20. Linden, J., et al., *Precision in 2D temperature measurements using the thermographic phosphor BAM*. *Measurement Science & Technology*, 2012. **23**(8).
21. Bizarri, G. and B. Moine, *On BaMgAl<sub>10</sub>O<sub>17</sub>:Eu<sup>2+</sup> phosphor degradation mechanism: thermal treatment effects*. *Journal of Luminescence*, 2005. **113**(3-4): p. 199-213.
22. Lacanilao, A., et al., *Structural analysis of thermal degradation and regeneration in blue phosphor BaMgAl<sub>10</sub>O<sub>17</sub>:Eu<sup>2+</sup> based upon cation diffusion*. *Solid State Ionics*, 2013. **253**: p. 32-38.
23. Hiroswawa, I., et al., *Oxidation of doped europium in BaMgAl<sub>10</sub>O<sub>17</sub> by annealing studied by x-ray-absorption fine-structure measurements*. *Journal of the Society for Information Display*, 2004. **12**(3): p. 269-273.
24. Yang, P., G.-Q. Yao, and J.-H. Lin, *Energy transfer and photoluminescence of BaMgAl<sub>10</sub>O<sub>17</sub> co-doped with Eu<sup>2+</sup> and Mn<sup>2+</sup>*. *Optical Materials*, 2004. **26**(3): p. 327-331.
25. Shionoya, S. and W.M. Yen, *Phosphor handbook*. 1999: CRC Press.
26. Qiao, B., et al., *Study on ZnGa<sub>2</sub>O<sub>4</sub>:Cr<sup>3+</sup> a.c. powder electroluminescent device*. *Materials Letters*, 2007. **61**(2): p. 401-404.
27. Chao, C.-C., *Charge-transfer luminescence of Cr<sup>3+</sup> in magnesium oxide*. *Journal of Physics and Chemistry of Solids*, 1971. **32**(11): p. 2517-2528.
28. Wojtowicz, A., *Luminescence of Cr<sup>3+</sup> in kyanite*. *Journal of Luminescence*, 1991. **50**(4): p. 221-230.
29. Pott, G. and B. McNicol, *Zero-Phonon Transition and Fine Structure in the Phosphorescence of Fe<sup>3+</sup> Ions in Ordered and Disordered LiAl<sub>5</sub>O<sub>8</sub>*. *The Journal of Chemical Physics*, 1972. **56**(11): p. 5246-5254.
30. Shannon, R., *Revised effective ionic radii and systematic studies of interatomic distances in halides and chalcogenides*. *Acta Crystallographica Section A: Crystal Physics, Diffraction, Theoretical and General Crystallography*, 1976. **32**(5): p. 751-767.
31. Kim, K.-B., et al., *Structural and optical properties of BaMgAl<sub>10</sub>O<sub>17</sub>:Eu<sup>2+</sup> phosphor*. *Chemistry of Materials*, 2002. **14**(12): p. 5045-5052.